International Immunopharmacology 75 (2019) 105797

Contents lists available at ScienceDirect

International Immunopharmacology

journal homepage: www.elsevier.com/locate/intimp

Scoparone alleviates inflammation, apoptosis and fibrosis of non-alcoholic steatohepatitis by suppressing the TLR4/NF-κB signaling pathway in mice

Beibei Liu[1], Xiaoling Deng[1], Qianqian Jiang, Guixin Li, Junli Zhang, Ning Zhang, Shengliang Xin, Keshu Xu*

Department of Gastroenterology, Union Hospital, Tongji Medical College, Huazhong University of Science and Technology, Wuhan 430022, China

ARTICLE INFO

Keywords:
Scoparone
Non-alcoholic steatohepatitis
Inflammation
Apoptosis
Fibrosis

ABSTRACT

Scoparone, a naturally-occurring, bioactive compound isolated from the Chinese herb Artemisia capillaria, has been shown to ameliorate hepatotoxicity and cholestasis in liver diseases. However, the pharmacological effect of scoparone in non-alcoholic steatohepatitis (NASH) has not been elucidated. In this study, we investigated the protective effects and mechanisms of scoparone in NASH. In vivo, the NASH model was established in mice fed a methionine and choline-deficient (MCD) diet for 4weeks, with or without simultaneous scoparone treatment. In vitro, RAW264.7 cells induced by lipopolysaccharide (LPS) were pretreated with or without different concentrations of scoparone. Hepatic triglycerides and serum AST and ALT levels were examined by biochemical assays. Hepatic histology was assessed by H&E, oil red O and Masson's trichrome staining methods, which were applied to analyze the protective effects of scoparone in NASH. To further explore the underlying mechanism of scoparone, immunohistochemistry, TUNEL, qRT-PCR, and Western blotting assays were applied to liver tissue or LPS-induced RAW264.7 cells. We found that scoparone can effectively improve hepatic steatosis, apoptosis, inflammation, and fibrosis in an MCD diet-induced NASH murine model. Mechanistically, we demonstrated that scoparone treatment alleviates NASH- and lipopolysaccharide (LPS)-induced immune responses in macrophages partly by blocking TLR-4/NF-κB signaling in a dose-dependent manner. Taken together, our results present the potential protective effects and mechanism of scoparone in NASH, suggesting a potentially beneficial drug treatment for NASH.

1. Introduction

With the current epidemic of obesity and diabetes, the morbidity of nonalcoholic fatty liver disease (NAFLD) is steadily increasing, and NAFLD is emerging as the most prevalent chronic liver disease worldwide [1]. NAFLD is defined as a clinicopathological syndrome, ranging from non-alcoholic fatty liver (NAFL) to nonalcoholic steatohepatitis (NASH), which is characterized by the appearance of lobular inflammation, hepatocyte ballooning and apoptosis, with or without fibrosis. As the progressive inflexion of worsening NAFLD, NASH can lead to cirrhosis and hepatocellular carcinoma (HCC) and increased mortality [2–4]. According to the “parallel, multiple-hit” hypothesis, the progression from NAFL to NASH is the consequence of multiple interactive factors, such as insulin resistance, lipotoxicity, oxidative stress, endoplasmic reticulum stress (ERS) and endotoxin from gut microbiota. Although these pathogenic molecular events, which converge on intracellular inflammatory signaling, may be potential therapeutic targets, there is still no effective pharmacologic treatment approved for NASH [5–9]. Therefore, there is an urgent need to find effective therapies to counteract NASH progression.

Inflammatory responses and accompanying fibrosis are key determinants of the long-term prognosis of NASH. Inflammatory cytokines and chemokines secreted by liver tissue are upregulated in NASH and then further recruit mononuclear macrophages of peripheral blood, initiating a cascade of immune responses. The polarization of macrophages toward a pro-inflammatory M1 phenotype is an important contribution to the progression of NASH [49]. As a classical inducer of macrophage activation and inflammation, serum lipopolysaccharide (LPS) is elevated due to intestinal microbiota dysbiosis in NASH patients [11]. Toll-like receptor 4 (TLR4), a pattern recognition receptor, recognizes LPS, which, in turn, recruits adaptor protein myeloid differentiation primary response gene 88 (MyD88) and activates downstream pro-inflammatory transcription factor nuclear factor-kappa B (NF-κB) [5,6,12]. In addition, upon continuous liver inflammation

* Corresponding author.
E-mail address: xl2017@hust.edu.cn (K. Xu).
[1] These two authors contributed equally to this work.

https://doi.org/10.1016/j.intimp.2019.105797
Received 25 April 2019; Received in revised form 10 July 2019; Accepted 31 July 2019
Available online 14 August 2019
1567-5769/

injury, hepatic stellate cells (HSCs) are activated to be the central factor causing hepatic fibrosis [6]. Therefore, drugs targeting the TLR4/MyD88/NF-κB signaling pathway may be a potential therapy for NASH.

Scoparone (6,7-Dimethoxycoumarin,molecular formula, C11H10O4, Fig. S1), a naturally-occurring bioactive compound isolated from the Chinese herb Artemisia capillaris Thunb (also known as Yinchenhao), has multiple pharmacological properties, including anti-allergenic, hypolipidemic, anti-hypertensive, anti-inflammatory and anti-tumor properties [13–17]. In China, Yinchenhao has been a classic potion for 1800 years, traditionally used to treat liver and choleretic disorders. Currently, it is still applied for the treatment of acute jaundice hepatitis and other liver disease [18]. It was reported that scoparone had hepatoprotective effects both on alcoholic-induced hepatotoxicity and carbon tetrachloride (CCL4)-induced liver damage in rats [19–21] by potentiating transactivation of the bile salt export pump gene (BSEP) both in mice and cultured cells transfected with human BSEP promoter [22] and by attenuating the activation of HSCs by suppressing TGF-β/Smad signaling pathway [23]. Importantly, a previous study on the pharmacokinetics and tissue distribution of scoparone in rats indicated that after oral administration, scoparone had the highest level of distribution in the liver [24]. However, the effects and underlying molecular mechanisms of scoparone in NASH and macrophages are unknown.

In the present study, we investigated the effects and potential mechanisms of scoparone on methionine and choline deficient (MCD) diet-induced NASH in mice and RAW264.7 macrophages induced by LPS. Our results demonstrated that scoparone can improve inflammation, apoptosis and fibrosis in NASH partly by inhibiting the activation of the TLR4/NF-κB signaling pathway.

2. Materials and methods

2.1. Reagents and antibodies

Scoparone (HPLC ≥ 98%, CAS number: 120-08-1, endotoxin-free) was purchased from Dalian Meilun Biology Technology Co. Ltd. (Dalian, China). Dimethyl sulfoxide (DMSO), LPS from E. coli 0111:b4 (cat. no.L2630), and corn oil were obtained from Sigma-Aldrich (Merck KGaA, Darmstadt, Germany). Dulbecco's modified Eagle's medium (DMEM) and fetal bovine serum (FBS) were purchased from Gibco (Thermo Fisher Scientific, Inc., Waltham, MA, USA). Information on the primary antibodies is shown in Table S1. Secondary antibodies labeled with horseradish peroxidase (HRP, Western blot) were purchased from Antgene Biotechnology Co., Ltd. (Wuhan, China). For the animal experiments, scoparone was dissolved in 10% DMSO diluted with corn oil immediately before intraperitoneal injection in mice. For the cellular experiments, scoparone (200 mM) was dissolved in DMSO stored at −20 °C and diluted in culture medium with a final concentration of 0.1% DMSO.

2.2. Animals and treatments

C57BL/6 mice (male, 6-week-old, 18–20 g) and an MCD diet (cat. no.H10401) were purchased from Huafukang Bioscience Co. Inc. (Beijing, China). The mice were housed in a standard 12 h light/dark cycle environment with controlled temperature (22 ± 2 °C) and humidity (40%–60%) and received food and drinking water ad libitum in specific pathogen-free (SPF) laboratory animal rooms. After an acclimatization period of one week, mice were randomly divided into six groups (n = 6/group)with daily intraperitoneal injection as follows: (1) Chow diet group (CD): mice were fed a chow diet treated with vehicle (10% DMSO in corn oil, which was reported to be suitable for in vivo usage in mice [25,26]); (2) Scoparone group (SC): mice were fed a chow mice diet treated with80 mg/kg scoparone; (3) MCD diet group (MCD): mice were fed an MCD diet treated with vehicle; (4) Low-dose scoparone (SC-L): mice were fed an MCD diet treated with 20 mg/kg scoparone; (5) Middle-dose scoparone group (SC-M): mice were fed an MCD diet treated with 40 mg/kg scoparone; (6) High-dose scoparone (SC-H): mice were fed an MCD diet treated with 20 mg/kg scoparone. The scoparone dosing strategies were designed according to previous studies with minor modifications [19,20,24]. The mice were weighed once a week and given the same volume of vehicle in the above mentioned groups for 4 weeks. Then, mice were sacrificed under chloral hydrate after an overnight fast. The fresh liver tissues were collected and stored at −80 °C for molecular biological assays. The serums were isolated from heart blood samples by centrifugation at 3000 × *g* for 15 min at 4 °C for the detection of serum transaminase. In addition, the partial hepatic tissues were fixed with 4% paraformaldehyde for histological examination. The animal study described above was approved by the Animal Research Ethics Committee of Tongji Medical College, Huazhong University of Science and Technology.

2.3. Cell culture and treatments

RAW264.7 cells (mouse mononuclear macrophage line) were cultured in DMEM medium supplemented with 10% FBS and incubated at 37 °C in a humid atmosphere containing 5% CO2. Cells were gently scraped for passage with a cell scraper and maintained healthy growth in the logarithmic phase. RAW264.7 cells were pretreated with scoparone with progressive concentrations (25, 50, 100, and 200 μM) for 2 h and then incubated with LPS (1 μg/ml) for an additional 16 h. Cells in all wells were treated with an equal volume of 0.1% DMSO, which also served as a control.

2.4. Biochemical assays: liver TG and serum ALT and AST

The mouse serum levels of alanine aminotransferase (ALT) and aspartate aminotransferase (AST) were measured using commercial reagent kits by the microplate method, according to the manufacturer's instructions. The liver triglyceride (TG) levels of mice were measured using reagent kits by an enzymatic colorimetric method, according to the instructions. These reagent kits were obtained from Nanjing Jiancheng Bioengineering Institute (Nanjing, China).

2.5. H&E and oil red O staining analysis

Liver tissues were fixed in 4% paraformaldehyde, embedded in paraffin, sectioned into 4 μm slices and stained with hematoxylin and eosin (H&E). Histological scoring of the liver lesions was evaluated by NAFLD activity score (NAS), which was calculated as the unweighted sum of the scores for steatosis (0–3), lobular inflammation (0–3), and ballooning (0–2), and ranged from 0 to 8. Liver tissue samples with scores ≥ 5 were diagnosed as “NASH”, and samples with scores ≤ 2 were diagnosed as “not NASH” [27,28]. For oil red O staining, 8-μm-thick frozen liver sections were fixed in 4% paraformaldehyde for 10 min, washed with deionized water 3 times and stained with oil red O working solution (Sigma-Aldrich) for 10 min at room temperature, washed in deionized water and stained with hematoxylin.

2.6. Immunohistochemistry analyses

Paraffin-embedded liver sections (4 μm thick) were dewaxed and sequentially incubated with anti-F4/80 and anti-a-SMA primary antibodies and biotinylated secondary antibody (Proteintech, Wuhan, China). Positive staining was detected by using DAB chromogenic agent, and then all sections were counterstained with hematoxylin. For quantification of the positive staining area, five random fields were selected from each stained section and analyzed using Image J V1.8.0 software (National Institute of Health).

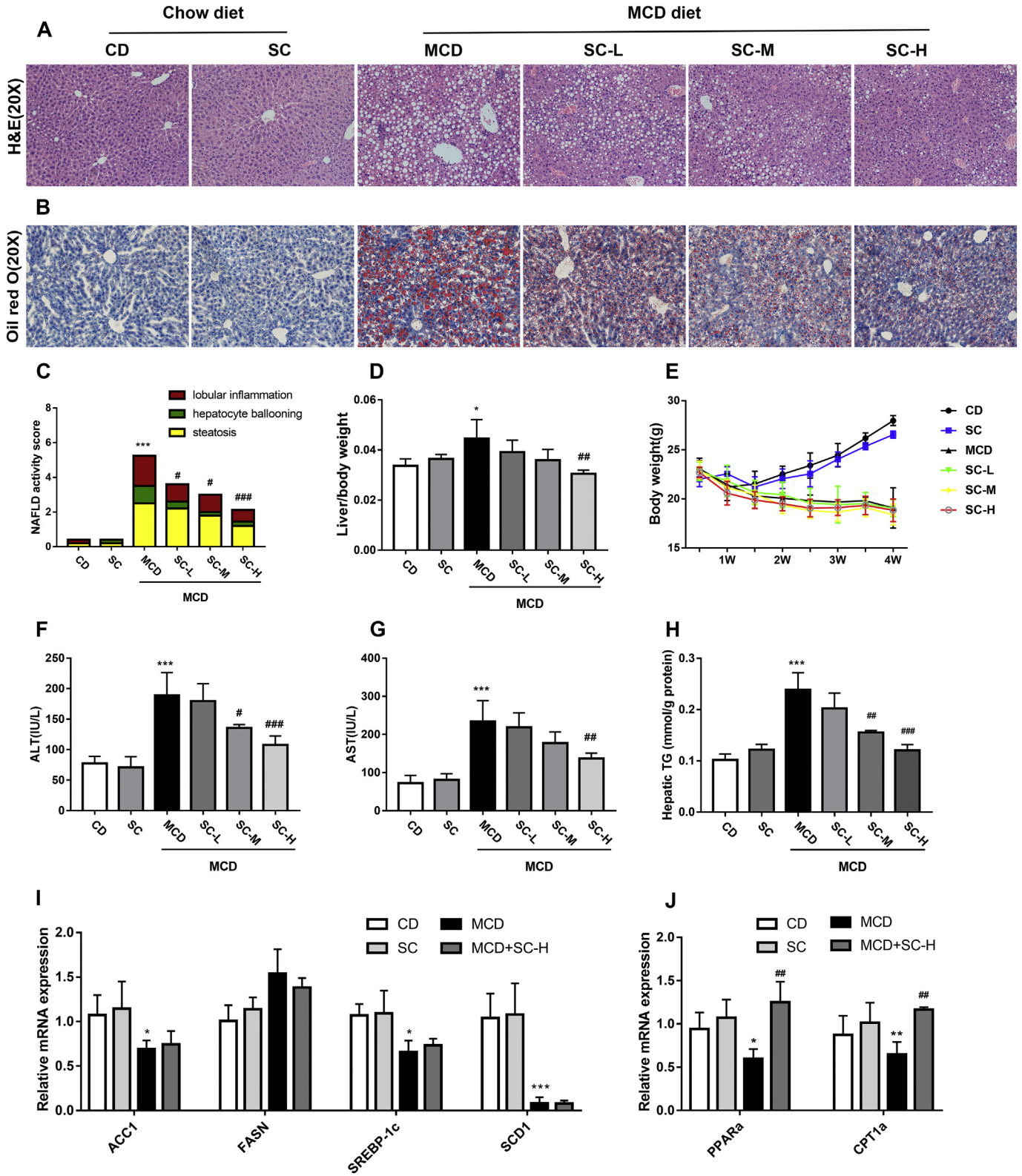

Fig. 1. Scoparone attenuates liver steatosis and injury in mice induced by an MCD diet. Mice were divided into six groups (CD, SC, MCD, SC-L, SC-M, SC-H) and treated as described in "2.2 Animals and treatments". (A–B) Representative images of H&E staining and oil red O staining from each group. (C) The histological NAS of steatosis, hepatocyte ballooning and lobular inflammation. (D) The ratio of liver/body weight. (E) The curve of the body weight of the mice during feeding. (F-H) Serum levels of ALT, AST and hepatic TG content. (I–J) The mRNA levels of ACC1, FASN, SREBP-1c, SCD1, PPARa and CPT1a were determined by qRT-PCR in mouse liver samples. n = 5–6 mice/group. Data are shown as the mean ± SD, $^{*}p < 0.05$, $^{**}p < 0.01$, $^{***}p < 0.001$ vs CD group; $^{\#}p < 0.05$, $^{\#\#}p < 0.01$, $^{\#\#\#}p < 0.001$ vs MCD group.

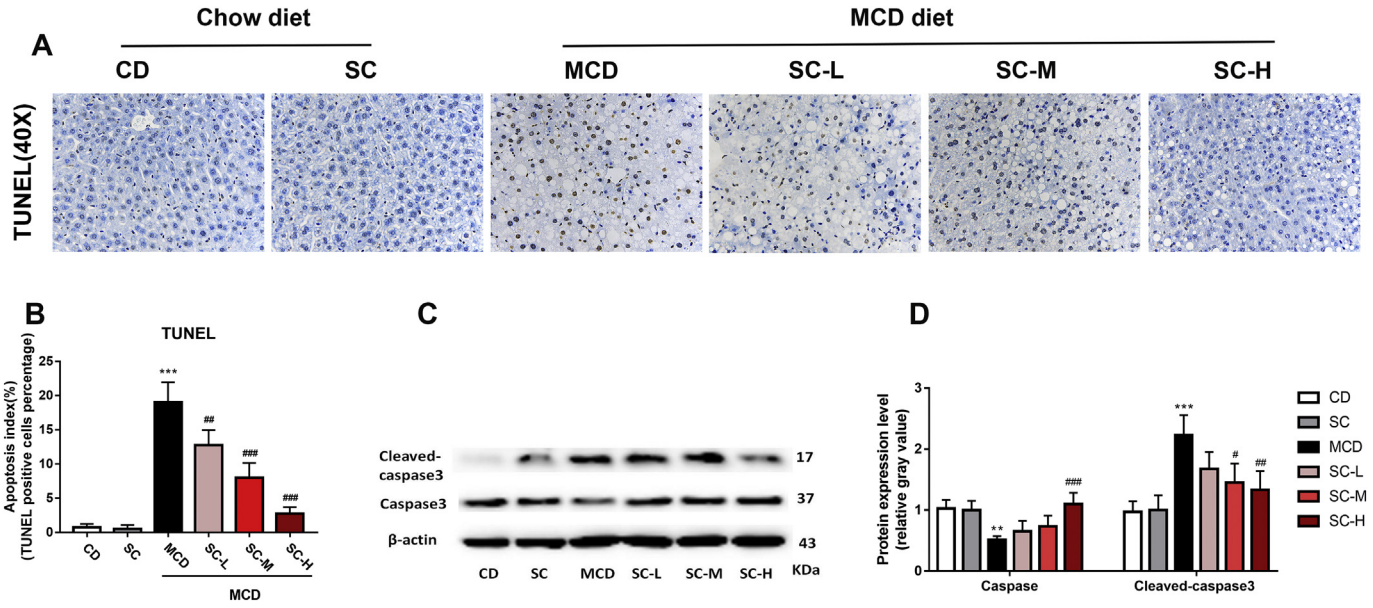

Fig. 2. Scoparone reduces hepatocyte apoptosis induced by an MCD diet in mice. (A) Representative images of the TUNEL assay from each group. (B) Quantification of the apoptotic index is shown by the percentage of TUNEL-positive cells (brown nucleus) in liver sections. (C–D) The protein levels of cleaved-caspase-3 and caspase-3 were evaluated by Western blot in liver samples. n = 5/group. Data are shown as the mean ± SD, $^{*}p < 0.05$, $^{**}p < 0.01$, $^{***}p < 0.001$ vs CD group; $^{\#}p < 0.05$, $^{\#\#}p < 0.01$, $^{\#\#\#}p < 0.001$ vs MCD group. (For interpretation of the references to colour in this figure legend, the reader is referred to the web version of this article.)

2.7. Masson and TUNEL assays

Paraffin-embedded liver tissues were sliced into 4 μm-thick sections and stained with Masson's trichrome. In brief, liver sections were dewaxed and then stained nuclei with hematoxylin; cytoplasm was stained with a mix of xylidine ponceau and acid fuchsin; and collagen fiber was stained with anilin blue. To quantify the blue staining area of collagen fiber, five random fields were selected from each stained section and analyzed using Image J software. Apoptosis was detected by terminal deoxynucleotidyl transferase-mediated dUTP nick-end labeling (TUNEL) assay, and liver paraffin sections were obtained according to the instructions of the In Situ Cell Death Detection kit (Roche Diagnostics GmbH, Mannheim, Germany). Images were acquired on an optical microscope at 40× magnification. TUNEL-positive nuclei of five random fields per section were counted by Image J V1.8.0 software (National Institute of Health).

2.8. Cell proliferation assay

Cell proliferation was measured using cell counting kit-8 (CCK-8) (Dojindo Chemical Technology Co., Ltd. Shanghai, China). In brief, RAW264.7 cells were seeded into 96-well plates at a density of 1×10^5 cells/ml and cultured for 24 h. Then, the cells were treated with various concentrations of scoparone (25, 50,100, 200, 400 μM) or an equal volume of DMSO for 24 h. In the LPS-intervention groups, cells were pretreated with scoparone (25, 50, 100, and 200 μM) for 2 h and exposed to LPS (1 μg/ml) for an additional 16 h. Then, 10 μl of CCK-8 reagent was added to each well and incubated with cells for 2 h in a 37 °C incubator. The absorbance was assessed at 450 nm using a microplate reader (BioTek Instruments, Inc., Winooski, VT, USA).

2.9. Protein extraction and Western blot assay

Protein extraction and Western blot were performed as described previously [29]. In brief, total protein samples were extracted by treating liver tissues or cells with RIPA lysis buffer and protease inhibitor cocktail tablets, and protein concentrations were measured. Denatured proteins were separated by SDS-PAGE and transferred to polyvinylidene difluoride (PVDF) membranes (Millipore Corp., Billerica, MA, USA). The membranes were blocked and incubated with specific primary antibodies (Table S1) overnight at 4 °C. Then, the membranes were incubated with secondary antibodies, and immunoreactive protein bands were visualized with the enhanced chemiluminescence (ECL) kit (Beyotime, China).

2.10. RNA extraction and quantitative real-time PCR

Total RNA from RAW264.7 cells and liver tissues was isolated with RNAiso Plus reagent and reverse transcribed to cDNA using a PrimeScript™ RT Master Mix according to the manufacturer's protocol (Takara Biomedical Technology Co. Ltd., Beijing, China). The sequences of the primers are listed in Table S2.Quantitative real-time polymerase chain reaction (qRT-PCR) was performed with SYBR Premix Ex Taq™ (Takara, China)using the LightCycler 480 Software (Roche Diagnostics GmbH, Mannheim, Germany). The qRT-PCR cycling parameters were 95 °C for 5 min, followed by40 cycles of 95 °C for 5 s and 60 °C for 30 s. The relative expression levels were calculated by the $2^{-\Delta\Delta Ct}$ method using GAPDH as a control.

2.11. Statistical analysis

Statistical analysis was performed with GraphPad Prism 7(GraphPad Software Inc., La Jolla, CA, USA). Statistical differences between data of multiple groups were analyzed by one-way analysis of variance (ANOVA). Numerical data are presented as the mean ± standard deviation (SD). $P < 0.05$ was considered statistically significant.

3. Results

3.1. Scoparone attenuates MCD-induced liver steatosis and injury in mice

To investigate the potential effect of scoparone on NASH, C57BL/6 mice were fed either a CD or MCD diet for 4 weeks. As expected, MCD-induced mice exhibited a significant reduction in body weight and a higher ratio of liver/body weight, while scoparone treatment reduced

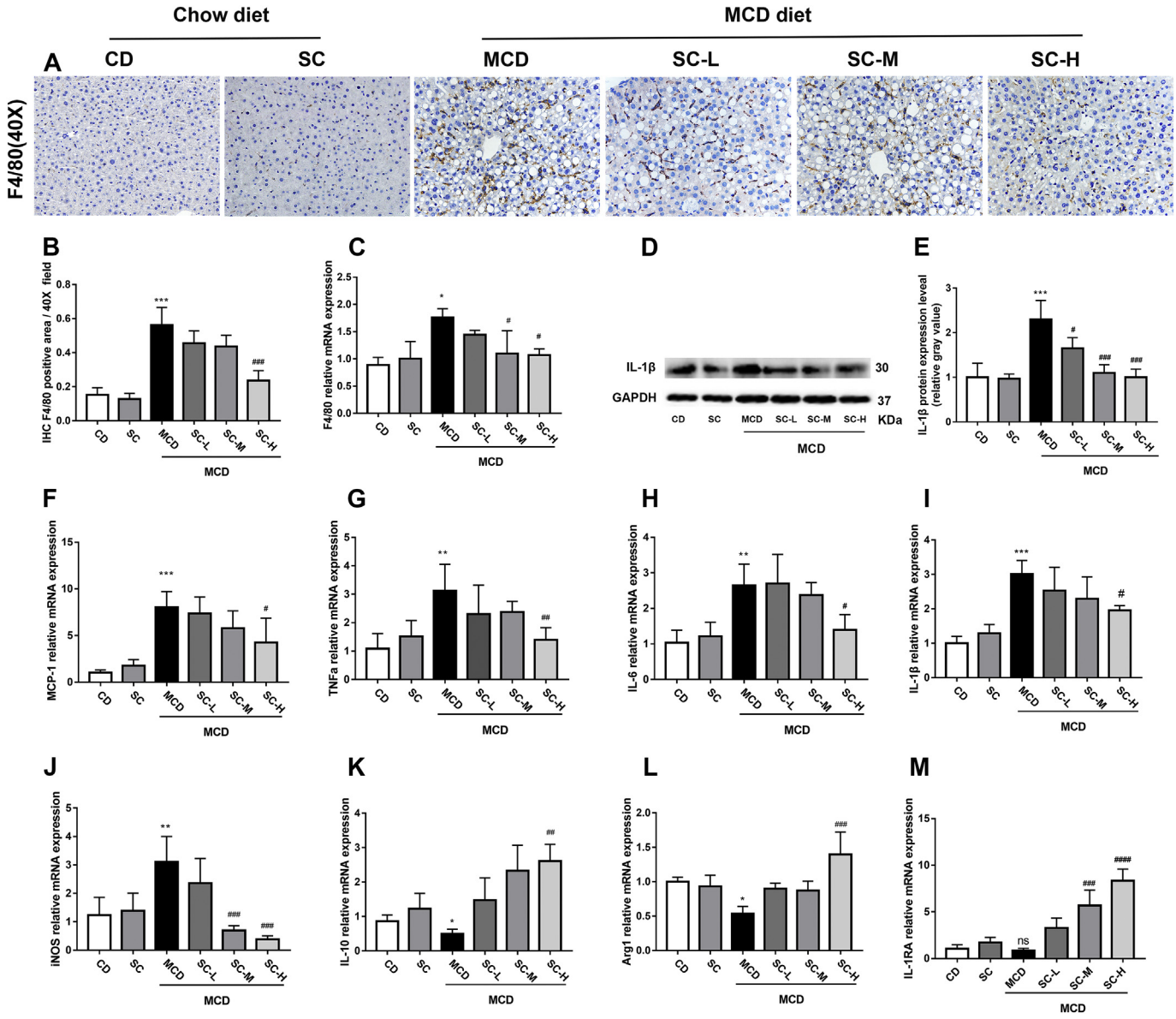

Fig. 3. Scoparone relieves inflammation induced by an MCD diet in mice. (A) Representative images of F4/80 immunohistochemical (IHC) staining in liver samples. (B) Quantification of F4/80 IHC-positive staining area is shown (n = 5 mice/group). (C–D) The protein levels of IL-1β were evaluated by Western blot in liver samples (n = 5/group). (E–J) The mRNA levels of the pro-inflammatory cytokines IL-1β, MCP-1, TNF-α, F4/80, and iNOS were determined by qRT-PCR in mouse liver samples (n = 5–6 mice/group). (K-M) The mRNA levels of the anti-inflammatory cytokines IL-10, Arg1 and IL-1RA were determined by qRT-PCR in mouse liver samples (n = 5–6 mice/group). Data are shown as the mean ± SD. $^{*}p < 0.05$, $^{**}p < 0.01$, $^{***}p < 0.001$ vs CD group; $^{\#}p < 0.05$, $^{\#\#}p < 0.01$, $^{\#\#\#}p < 0.001$ vs MCD group.

the liver/body weight ratio (Fig. 1D, E).

Histological H&E and oil red O staining showed that the MCD diet triggered obvious hepatic macrovesicular steatosis and inflammatory cell infiltration in mice compared with CD-fed mice. However, scoparone treatment ameliorated the number and size of lipid droplets, inflammatory foci (Fig. 1A, B) and hepatic TG content (Fig. 1H). In addition, the increased NAFLD activity score (NAS), calculated by steatosis, hepatocyte ballooning and lobular inflammation, was significantly decreased by scoparone supplementation according to histological evaluation of the liver (Fig. 1C). Consistent with the histologic findings, distinct hepatocyte damage, reflected by increased serum ALT and AST levels, was also induced by the MCD diet. However, scoparone treatment significantly reduced the increased levels of ALT and AST in a dose-dependent manner in MCD-induced mice (Fig. 1F, G). Notably, there were no obvious changes in hepatic histology and serum transaminase levels in scoparone (80 mg/kg)-treated mice fed a chow diet (SC group), suggesting that scoparone has no obvious side effects of hepatotoxicity in normal mice.

We next examined the possible mechanism of scoparone in lipid metabolism. Despite no effect on lipid synthesis genes, *SREBP-1c*, *AAC1*, *FASN* and *SCD1*, scoparone intervention markedly reversed the expression of hepatic genes in fatty acid (FA) β-oxidation, *PPARα*, and the downstream target gene *CPT1a*, which was inhibited by the MCD diet in mice (Fig. 1I, J).

3.2. Scoparone reduces hepatocyte apoptosis induced by an MCD diet in mice

Next, we explored the potential mechanism of scoparone in improving hepatic injury. A previous study demonstrated that enhanced hepatocyte apoptosis is a key mechanism accelerating inflammation and fibrogenesis in NASH [30]. Here, we investigated the effect of

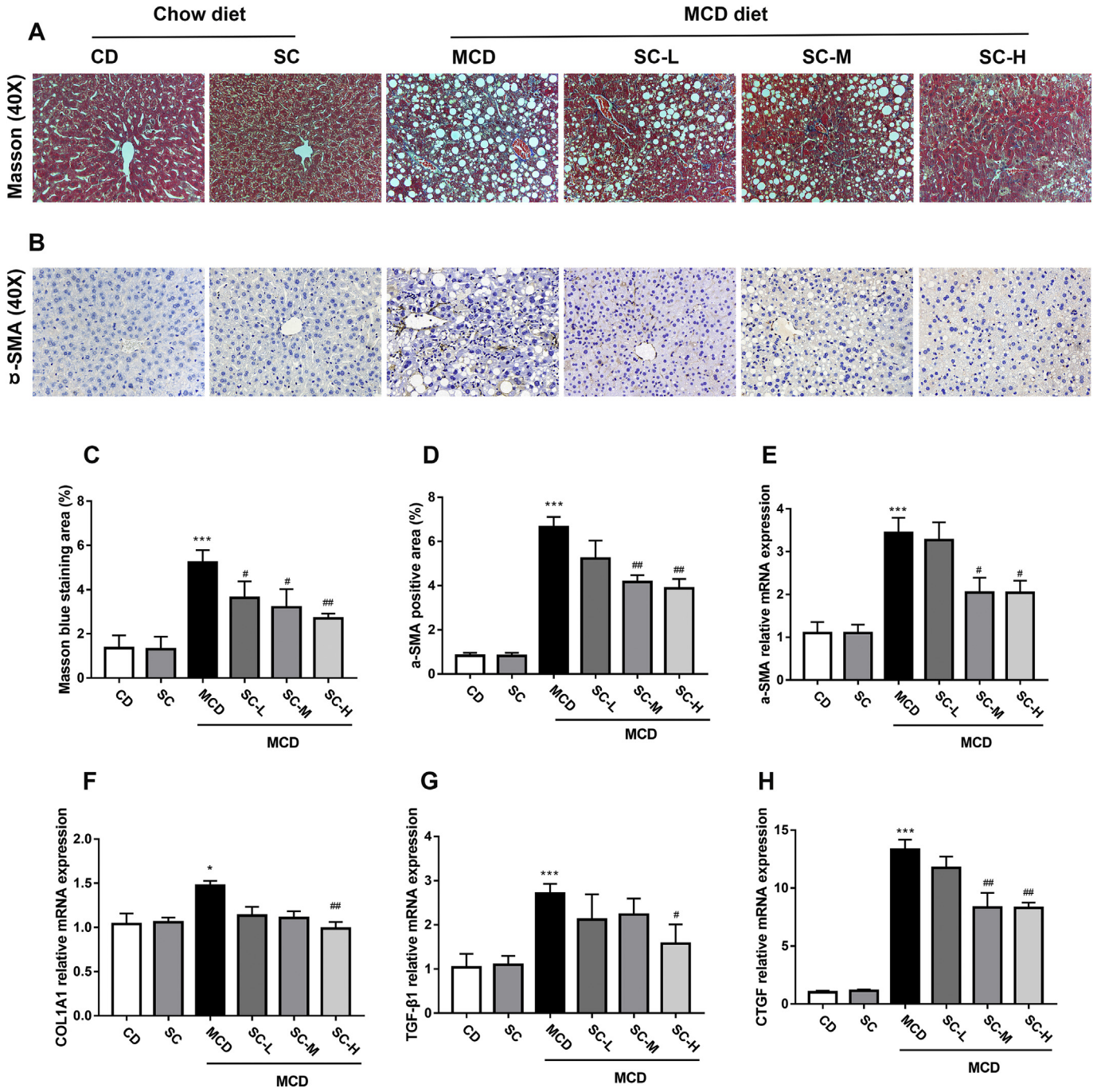

Fig. 4. Scoparone ameliorates fibrosis induced by an MCD diet in mice. (A, C) Representative images of Masson trichrome staining in liver sections (A) and quantification of collagen fiber staining (blue staining area) (C) (n = 5 mice/group). (B, D) Representative images of immunohistochemical (IHC) staining of a-SMA in the indicated groups (B) and quantification of a-SMA IHC-positive staining area (D) (n = 5 mice/group). (E–H) The mRNA levels of a-SMA, TGF-β1 and CTGF were determined by qRT-PCR in mouse liver samples (n = 5–6 mice/group). Data are shown as the mean ± SD, $^{***}p < 0.001$ vs CD group; $^{\#}p < 0.05$, $^{\#\#}p < 0.01$, $^{\#\#\#}p < 0.001$ vs MCD group. (For interpretation of the references to colour in this figure legend, the reader is referred to the web version of this article.)

scoparone on inhibiting hepatocyte apoptosis by TUNEL assay and determined the cleaved caspase-3 expression. A markedly increased percentage of TUNEL-positive cells induced by the MCD diet was observed, but it was significantly decreased in mice administered scoparone (Fig. 2A, B). A similar trend was observed in the hepatic expression of cleaved-caspase-3, a major terminal shear enzyme in apoptosis (Fig. 2C, D).

3.3. Scoparone relieves inflammation of MCD-induced NASH in mice

It is well acknowledged that the accumulation of macrophages, including local Kupffer cells and circulating monocyte-derived macrophages, and the overproduction of pro-inflammatory cytokines are vital pathological characteristics of NASH [31]. Consistent with the histopathological signs of inflammation in NASH, we found that the expression of F4/80, a marker of macrophage infiltration, was significantly upregulated in MCD-fed mice, while its expression was markedly downregulated in MCD-fed mice supplemented with

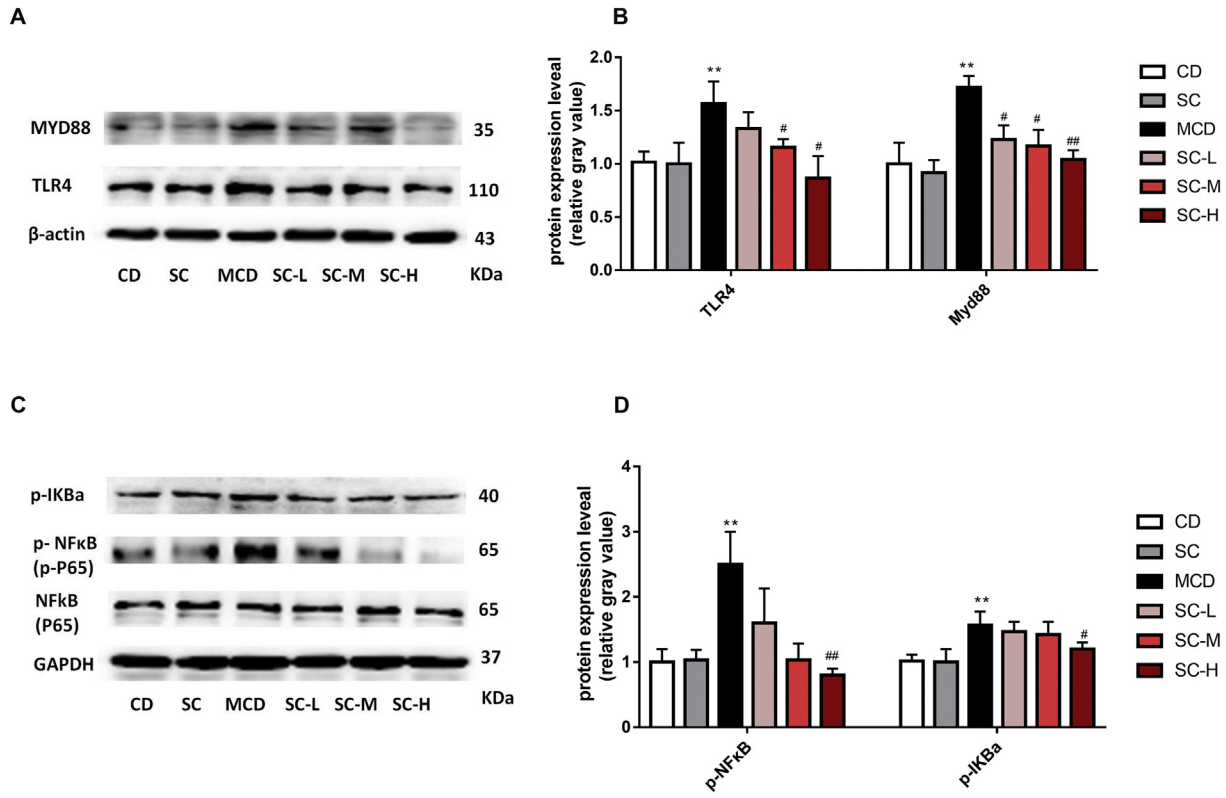

Fig. 5. Scoparone blocks the TLR4/NF-κB signaling pathway in the liver of mice with NASH induced by an MCD diet. (A–B) The protein levels of MyD88 and TLR4 were evaluated by Western blot in liver samples from the indicated groups. (C–D) The protein levels of total p65, phosphorylated p65 and IκBα were evaluated by Western blot in liver samples. n = 5 mice/group. Data are shown as the mean ± SD, $^{**}p < 0.01$ vs CD group; $^{\#}p < 0.05$, $^{\#\#}p < 0.01$ vs MCD group.

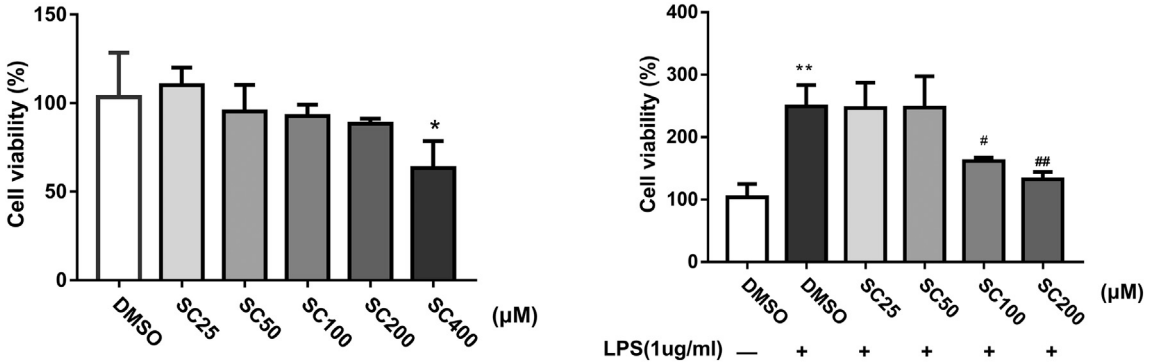

Fig. 6. Effects of scoparone on cell proliferation in RAW264.7 cells. (A) Cells were treated with the indicated concentrations of scoparone or an equal volume of DMSO for 24 h. (B) Cells were pretreated with the indicated concentrations of scoparone or an equal volume of DMSO for 2 h and then exposed to LPS (1 μg/ml) for 16 h. $^{*}p < 0.05$, $^{**}p < 0.01$ vs DMSO group; $^{\#}p < 0.05$, $^{\#\#}p < 0.01$ vs DMSO + LPS group.

scoparone (Fig. 3A–C). We also found that the hepatic mRNA levels of pro-inflammatory cytokines MCP-1, TNF-α, IL-6, IL-1β and iNOS were obviously increased in mice fed the MCD diet but reduced by treatment with scoparone in a dose-dependent manner (Fig. 3F–I). Corresponding to these results, the decreased expression of anti-inflammatory cytokines IL-10, Arg1 and IL-1RA in MCD-fed mice was upregulated by scoparone treatment (Fig. 3K–M). The downregulation of IL-1β expression levels by scoparone treatment was also demonstrated by Western blot assay (Fig. 3D, E).

3.4. Scoparone ameliorates NASH-related fibrosis induced by an MCD diet in mice

To further investigate the effects of MCD diet and scoparone on fibrosis in mice, histological assays with Masson trichrome staining and immunostaining of a-SMA were performed. As expected, the mice fed the MCD diet showed collagen deposition by Masson trichrome staining. However, scoparone treatment significantly reduced collagen deposition (Fig. 4A, C). Consistently, the increases in positive immunostaining of a-SMA, a marker of activated HSCs, were suppressed in MCD-fed mice treated with scoparone (Fig. 4B, D). Additionally, the hepatic mRNA expression of pro-fibrotic markers α-SMA, COL1A1 TGF-β1 and CTGF was enhanced in MCD diet-fed mice and attenuated by scoparone treatment (Fig. 4E–H).

3.5. Scoparone blocks the hepatic TLR4/NF-κB signaling pathway in mice with NASH induced by an MCD diet

We next explored the underlying molecular mechanism of the protective effects of scoparone on MCD-induced NASH. TLR4/NF-κB

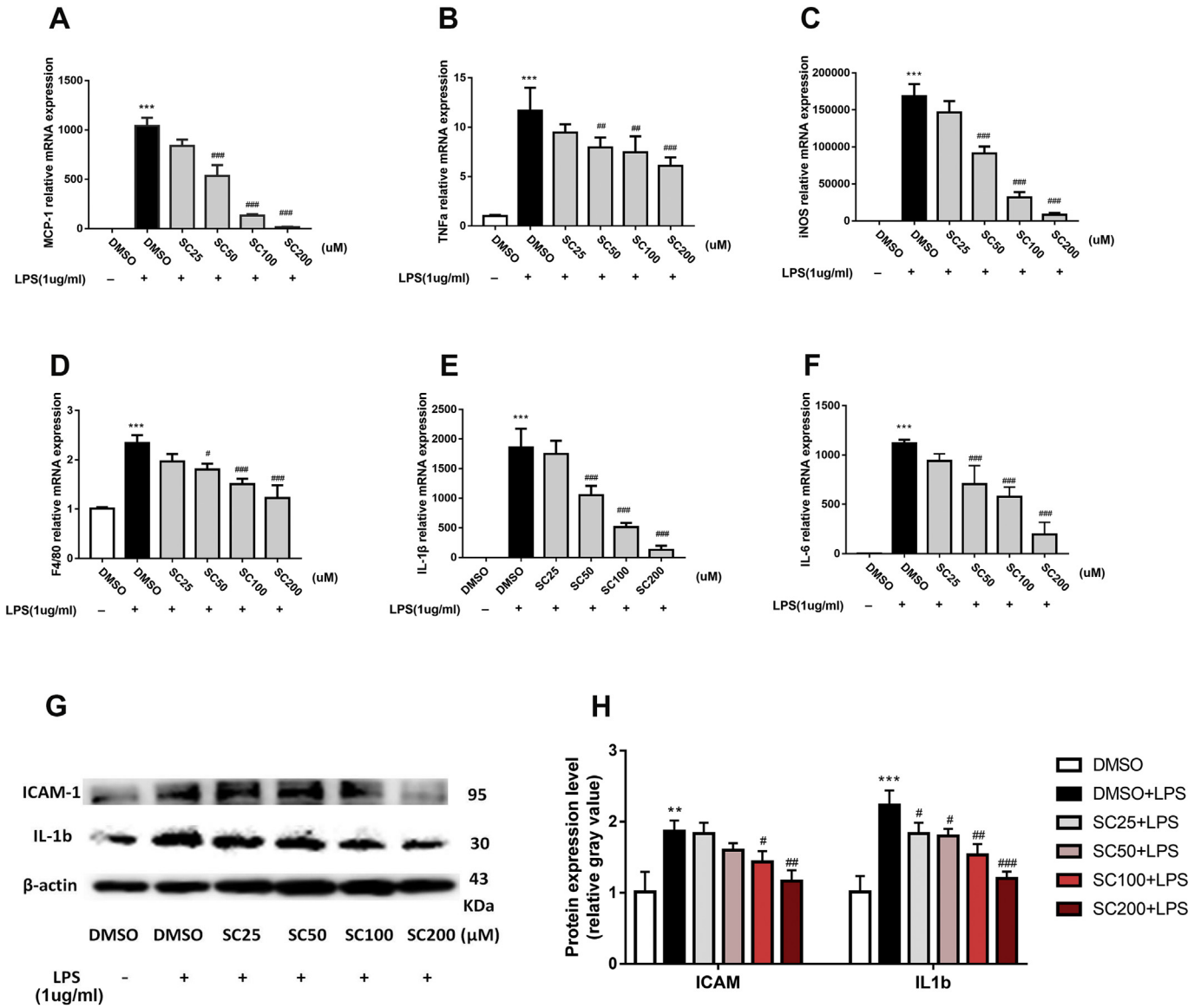

Fig. 7. Scoparone inhibits the expression of proinflammatory cytokines in RAW264.7 cells stimulated by LPS. (A–F) The mRNA levels of MCP-1, TNF-α, iNOS, F4/80, IL-1β, and IL-6 were determined by qRT-PCR in RAW264.7 cells. (G–H) The protein levels of IL-1β and ICAM1 were evaluated by Western blot in RAW264.7 cells. Data are from at least three independent experiments and shown as the mean ± SD; $^{*}p < 0.05$, $^{**}p < 0.01$, $^{***}p < 0.001$ vs DMSO group; $^{\#}p < 0.05$, $^{\#\#}p < 0.01$, $^{\#\#\#}p < 0.001$ vs DMSO + LPS group.

signaling is known to be a critical factor in the pathogenesis of NASH in both damaged hepatocytes and activated hepatic macrophages [32]. We presumed that scoparone might play an anti-inflammatory role by inhibiting the TLR4/NF-κB pathway. As shown in Fig. 5, in the liver of mice, the MCD diet upregulated the protein expression of TLR4 and MyD88 and enhanced the phosphorylation of downstream NF-κB, but treatment with scoparone blocked those increase.

3.6. The effect of scoparone on cell proliferation of RAW264.7 mouse macrophages

The process of NASH development is accelerated due to activation of monocyte-derived macrophages in the liver, which are implicated in a secondary inflammatory response, and inhibition of monocyte macrophage recruitment could reduce steatohepatitis [33]. Thus, we next determined whether scoparone had an anti-inflammatory effect on activated RAW264.7 mouse macrophages and the underlying mechanism. First, we performed a CCK-8 assay to examine the effect of scoparone on cytotoxicity and proliferation in RAW264.7 cells. We observed that scoparone at concentrations of > 200 μM exhibited no cytotoxic effect on untreated macrophages (Fig. 6A). Therefore, we decided to choose the optimal concentrations of 25, 50, 100 and 200 μM scoparone for pretreatment in the following experiments. In addition, the proliferation of RAW264.7 cells markedly increased by LPS, which was apparently inhibited by scoparone supplementation (Fig. 6B). Hence, we surmised that scoparone repressed LPS-induced activation of RAW264.7 macrophages.

3.7. Scoparone inhibits the generation of pro-inflammatory cytokines in RAW264.7 cells with activation induced by LPS

Liver macrophages could tilt polarization toward anti-inflammatory M2 phenotype or pro-inflammatory M1 phenotype in the process of NAFLD [34][49]. To demonstrate the effect of scoparone on macrophage polarization, we further investigated the expression of inflammatory mediators. Similar to the results in vitro, the mRNA levels of pro-inflammatory cytokines and chemokines, MCP-1, TNF-α, iNOS, F4/80, IL-1β and IL-6 were increased in RAW264.7 cells incubated with

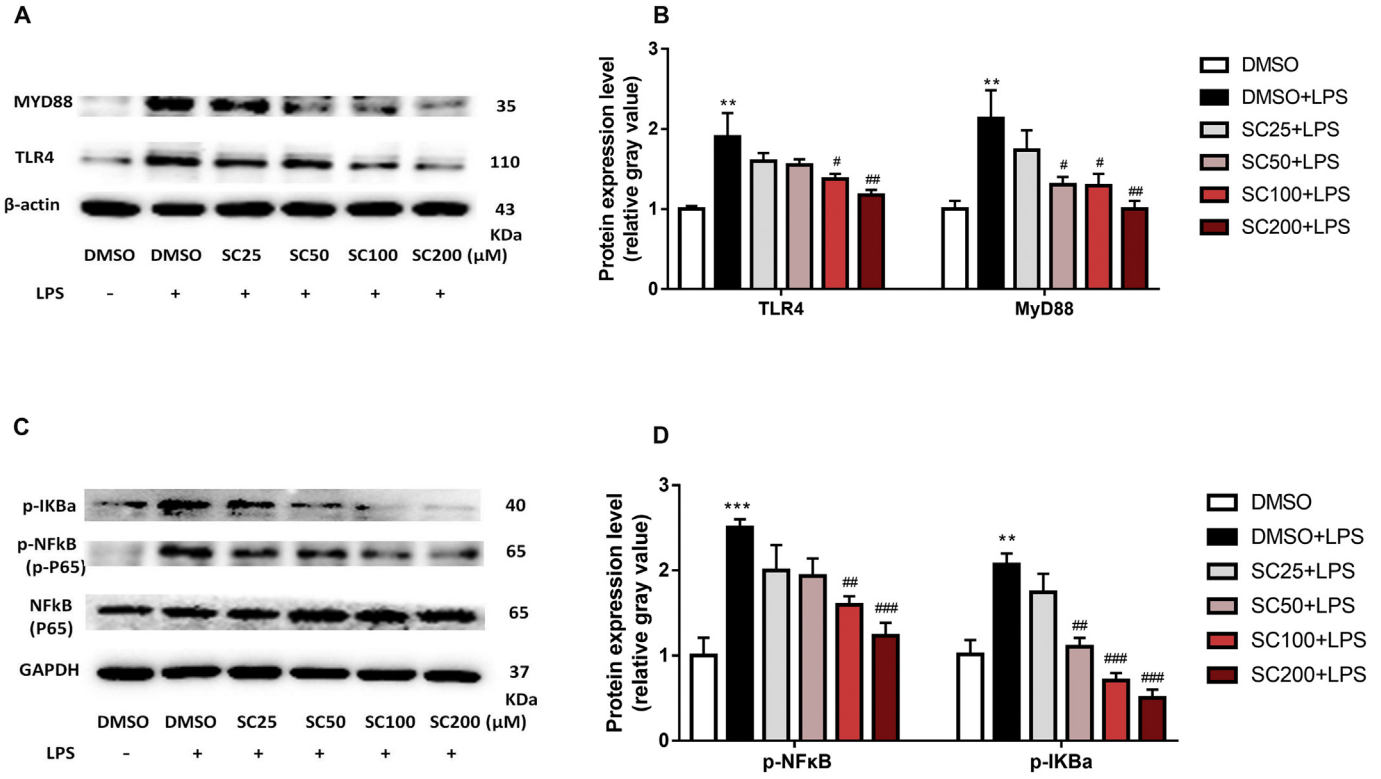

Fig. 8. Scoparone suppresses the TLR4/NF-κB signaling pathway in RAW264.7 cells stimulated by LPS. (A–D) The protein levels of MyD88, TLR4, IκBα, total p65 and phosphorylated p65 were evaluated by Western blot in RAW264.7 cells. Data are from at least three independent experiments and shown as the mean ± SD; $^{**}p < 0.01$, $^{***}p < 0.001$ vs DMSO group; $^{\#}p < 0.05$, $^{\#\#}p < 0.01$, $^{\#\#\#}p < 0.001$ vs DMSO + LPS group.

LPS, which indicates the M1 polarization of macrophages. The mRNA levels of these inflammatory mediators were significantly inhibited by scoparone pretreatment in a dose-dependent manner (Fig. 7A–F). Additionally, the downregulation of intercellular adhesion molecule 1 (ICAM1) and IL-1β by scoparone pretreatment was also confirmed by Western blot assay in LPS-treated RAW264.7 cells (Fig. 7G, H). The present results suggest that scoparone could markedly repress LPS-induced macrophage pro-inflammatory M1 polarization and thus be beneficial in ameliorating NASH.

3.8. Scoparone suppresses the TLR4/NFκB signaling pathway in RAW264.7 cells with activation induced by LPS

Considering the important relationship between LPS and the TLR4/NF-κB signaling pathway, we presumed that scoparone may attenuate pro-inflammatory cytokines by inhibiting the TLR4/NF-κB signaling pathway in LPS-induced macrophages. As shown in Fig. 8, our results are supported by the Western blot assay. The increased protein levels of TLR4 and MyD88 and the activity of downstream phosphorylated NF-κB stimulated by LPS were blocked by cotreatment with scoparone in RAW264.7 cells. All of these effects of scoparone in RAW264.7 cells were dose-dependent.

4. Discussion

NASH has become the major reason for chronic liver disease around the world. However, a large number of NASH patients are left with no effective treatment. In the current study, for the first time, we demonstrate that scoparone treatment modulates key events, including steatosis, hepatocyte apoptosis, inflammation, and fibrosis, in the pathogenesis of NASH in MCD-induced mice without obvious side effects. Our study also shows that the anti-inflammatory effect of scoparone is partly mediated by inhibiting the TLR4/NF-κB signaling pathway both in mice fed an MCD diet and in LPS-induced RAW264.7 macrophages.

In terms of the experimental model, mice fed the MCD diet rapidly developed clinicopathologic features of the progression from NAFL to NASH, such as severe inflammation, oxidative stress, apoptosis, and fibrogenesis [35,36]. Primarily, pathohistological features, the only gold standard for diagnosis of NASH, and serum transaminase were improved by scoparone treatment in mice fed the MCD diet. In the progression of NASH, lipid accumulation and impaired mitochondrial β-oxidation in the liver can lead to oxidative stress and then induce inflammatory responses and HSC activation [36]. Activation of PPARα-mediated FA β-oxidation and suppression of SREBP-1c-mediated lipogenesis are significant targets for NASH therapy [9]. Previously, scoparone was shown to inhibit TG accumulation in mature adipocytes and alcohol-induced changes in lipid metabolism in the primary hepatocytes of rats [20,37]. Consistent with those results, in the NASH mouse model induced by an MCD diet, we found that scoparone reduced hepatic lipid accumulation and reversed the decreased PPARα expression and its downstream gene CPT1a, which is involved in FA oxidation. However, no obvious change in the gene expression of lipogenesis (SREBP-1c and its target genes FASN and ACC1) was observed following scoparone treatment in the present study. This probably attributed to the mechanism of the MCD model, in which lipids are deposited in the liver due to impaired production and secretion of very low-density lipoprotein (VLDL) rather than increased lipogenesis [35]. According to the multiple-hit hypothesis, alleviation of hepatic steatosis by scoparone treatment is likely due to the suppression of hepatic oxidative stress, apoptosis and inflammation.

It has been proven that hepatocellular apoptosis is a critical mechanism that contributes to hepatic inflammation and fibrogenesis in NASH [30]. In the current study, we showed that scoparone treatment obviously lowered the amount of TUNEL-positive cells in liver tissue and inhibited the protein level of cleaved caspase-3. These results suggest that scoparone can ameliorate hepatocellular apoptosis

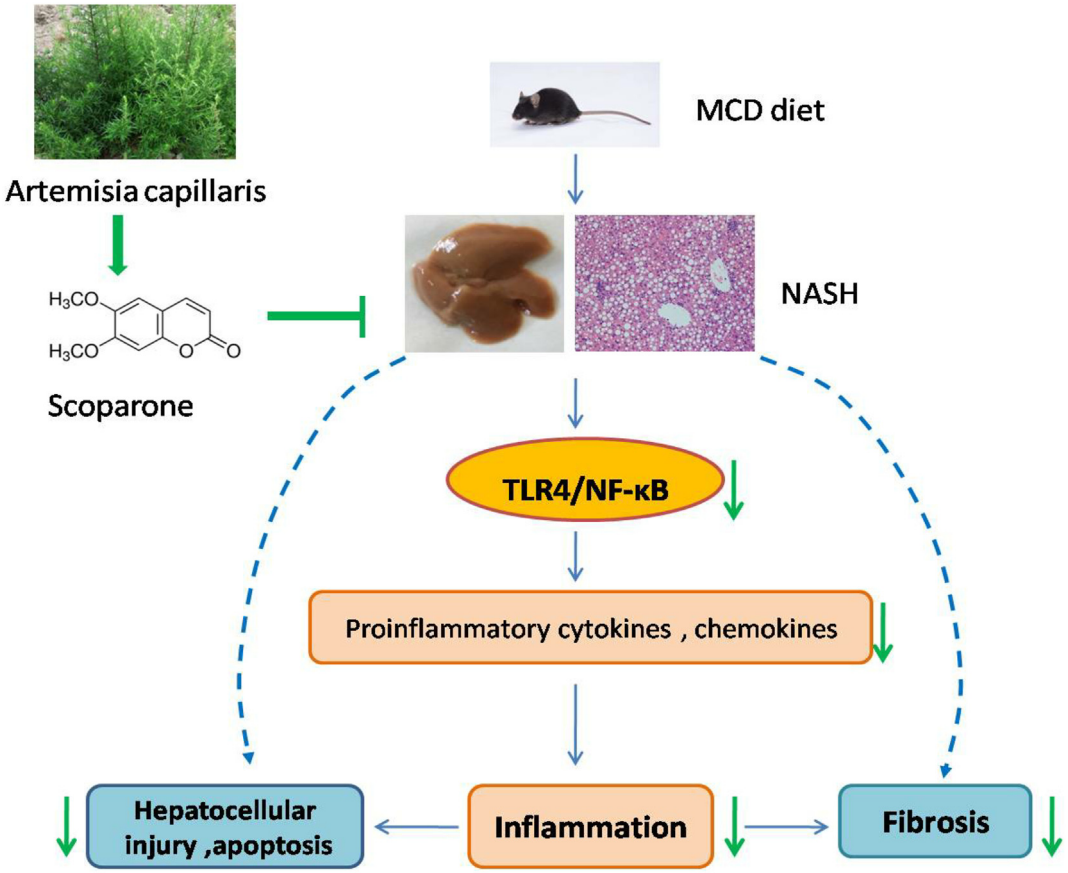

Fig. 9. Schematic representation illustrating the mechanism of scoparone in the improvement of NASH. Scoparone is a naturally-occurring bioactive compound isolated from Artemisia capillaria. Scoparone improves inflammation, apoptosis and fibrosis of NASH induced by an MCD diet in mice by inhibiting the TLR4/NF-κB pathway.

resulting from MCD diet-induced NASH in mice.

In addition, it is well known that mice fed an MCD diet exhibit enhanced inflammation by activation of NF-κB and concomitantly increased pro-inflammatory factors and chemokines and infiltration of activated macrophages into the liver [36]. NF-κB is a master regulator of the inflammatory response to hepatic injury in NASH. Furthermore, it has been well demonstrated that the TLR4/NF-κB signaling pathway activated by gut-derived LPS contributes to NASH progression by causing inflammatory liver damage [5,6,12]. Unsurprisingly, inhibition of NF-κB activation has been proven to exert therapeutic effects in several mouse models of NASH [38,39]. Recently, it was reported that scoparone could suppress the inflammatory response in LPS-simulated BV-2 microglial cells by inhibiting the IRF3/ERK signaling pathway and in IL-1b-induced human osteoarthritis chondrocytes through the PI3K/Akt/NF-kB signaling pathway [15,16]. Additionally, the study has previously stated that scoparone treatment inhibited the expression of TNF-a, IL-1b, IL-6, iNOS and COX-2 and prevented the production of NO and PGE2 in RAW264.7 cells stimulated by LPS; however, the exact molecular mechanisms remain under investigated [33]. In the current study, we detected that scoparone was capable of reducing serum transaminase, hepatic inflammation score and macrophage infiltration, which were elevated in mice fed an MCD diet. Specifically, scoparone attenuated the increased expression levels of pro-inflammatory mediators and the activation of the TLR4/MYD88/NF-κB signaling pathway in a dose-dependent manner in both liver tissue from MCD diet-induced NASH mice and LPS-stimulated RAW264.7 cells. These results suggest that scoparone has a potent anti-inflammatory effect on inflammatory models partly through the TLR4/NF-κB signaling pathway in vitro and in vivo. Moreover, infiltrating hepatic macrophages secrete pro-inflammatory cytokines such as IL-1β and TNF that perpetuate parenchymal damage by inducing apoptosis and encourage the progression of chronic liver injury and fibrosis through TGF-β/PDGF-mediated HSC transdifferentiation and proliferation [31,40].

Hepatic fibrosis, a reversible condition that puts a patient at great risk for cirrhosis, is a key histopathological feature in progressive NASH patients. HSC activation plays a critical role in liver fibrosis [6]. Recently, it was reported that scoparone could attenuate the proliferation and activation of TGF-β1-stimulated HSC-T6 cells by inhibiting the TGF-β/Smad signaling pathway [23]. Consistently, our current study indicates that scoparone ameliorates hepatic collagen deposition and the expression of profibrotic growth factors in liver tissue of mice fed an MCD diet. Thus, these results suggest that scoparone protects against NASH-related fibrosis by inhibiting HSC activation.

With the continued increase of theoretical and clinical studies of traditional Chinese medicine (TCM), Chinese herbal medicine is emerging with potential drug treatments for liver diseases [41]. Many natural herbal medicines have been demonstrated to be beneficial for improving NAFLD, such as silibinin, polydatin, cangju qinggan jiangzhi decoction and baicalin [42–45]. Silibinin, which modulates lipid homeostasis and is anti-inflammatory and anti-fibrotic for NASH [42,46,47], is suggested for clinical treatment of NASH in China [48]. As stated above, we first show the anti-inflammatory and hepatoprotective effects of scoparone on mice fed an MCD diet, suggesting that scoparone is a potentially beneficial drug for NASH (Fig. 9). Further studies of scoparone still need to be carried out to determine its clinical applications in the future.

Mice fed an MCD diet are considered a well-established NASH model with increased serum aminotransferase and hepatic histopathological features similar to human NASH, which is characterized by steatosis, hepatocyte ballooning and apoptosis, inflammation and

fibrosis. Nevertheless, a major disadvantage of this model is that the metabolic profile is opposite to that normally observed in NASH patients, such as weight loss instead of obesity, lack of peripheral insulin resistance, and reductions in plasma triglyceride and cholesterol levels instead of increases in these levels [36].Therefore, further investigations in high-fat and high-fructose models need to be carried out to confirm whether scoparone plays a protective role in obesity-induced NASH.

In summary, in the present study, we demonstrated that scoparone, isolated from the Chinese herb Artemisia capillaria, improved liver steatosis, inflammation, apoptosis and fibrosis of NASH in MCD-fed mice. In addition, we found that scoparone plays an anti-inflammatory role in both the NASH murine model and LPS-induced RAW264.7 cells partly through the TLR4/NF-κB signaling pathway. Our present study suggests that scoparone may be a promising agent for the treatment of NASH.

Author contributions

Beibei Liu and Xiaoling Deng, the co-first authors, designed and performed the experiments, collated and analyzed data, and wrote the manuscript. Qianqian Jiang, Guixin Li, Junli Zhang, Ning Zhang, and Shengliang Xin contributed to establishing the animal models, collected blood specimens or liver tissue samples, and participated in the discussion. Keshu Xu provided advice on the experimental design and modified the manuscript. All authors contributed to the manuscript.

Declaration of competing interest

The authors have declared that there are no conflicts of interest.

Acknowledgements

We are grateful for the grant support for this research from the National Natural Science Foundation of China (nos. 81670515 and 81370525).

Appendix A. Supplementary data

Supplementary data to this article can be found online at https://doi.org/10.1016/j.intimp.2019.105797.

References

[1] Z. Younossi, Q.M. Anstee, M. Marietti, T. Hardy, L. Henry, M. Eslam, E. Bugianesi, Global burden of NAFLD and NASH: trends, predictions, risk factors and prevention, Nat. Rev. Gastroenterol. Hepatol. 15 (1) (2018) 11–20, https://doi.org/10.1038/nrgastro.2017.109.

[2] L. Calzadilla Bertot, L.A. Adams, The natural course of non-alcoholic fatty liver disease, Int. J. Mol. Sci. 17 (5) (2016), https://doi.org/10.3390/ijms17050774.

[3] M.E. Rinella, Nonalcoholic fatty liver disease: a systematic review, Jama 313 (22) (2015) 2263–2273, https://doi.org/10.1001/jama.2015.5370.

[4] C. Alonso, D. Fernandez-Ramos, M. Varela-Rey, I. Martinez-Arranz, N. Navasa, S.M. Van Liempd, J.M. Mato, Metabolomic identification of subtypes of nonalcoholic steatohepatitis, Gastroenterology 152 (6) (2017) 1449–1461, https://doi.org/10.1053/j.gastro.2017.01.015.

[5] M.V. Machado, A.M. Diehl, Pathogenesis of nonalcoholic steatohepatitis, Gastroenterology 150 (8) (2016) 1769–1777, https://doi.org/10.1053/j.gastro.2016.02.066.

[6] F. Bessone, M.V. Razori, M.G. Roma, Molecular pathways of nonalcoholic fatty liver disease development and progression, Cell. Mol. Life Sci. (2018), https://doi.org/10.1007/s00018-018-2947-0.

[7] H. Tilg, A.R. Moschen, Evolution of inflammation in nonalcoholic fatty liver disease: the multiple parallel hits hypothesis, Hepatology 52 (5) (2010) 1836–1846, https://doi.org/10.1002/hep.24001.

[8] S.K. Mantena, A.L. King, K.K. Andringa, H.B. Eccleston, S.M. Bailey, Mitochondrial dysfunction and oxidative stress in the pathogenesis of alcohol- and obesity-induced fatty liver diseases, Free Radic. Biol. Med. 44 (7) (2008) 1259–1272, https://doi.org/10.1016/j.freeradbiomed.2007.12.029.

[9] G. Musso, M. Cassader, R. Gambino, Non-alcoholic steatohepatitis: emerging molecular targets and therapeutic strategies, Nat. Rev. Drug Discov. 15 (4) (2016) 249–274, https://doi.org/10.1038/nrd.2015.3.

[11] F. de Faria Ghetti, D.G. Oliveira, J.M. de Oliveira, L. de Castro Ferreira, D.E. Cesar, A.P.B. Moreira, Influence of gut microbiota on the development and progression of nonalcoholic steatohepatitis, Eur. J. Nutr. 57 (3) (2018) 861–876, https://doi.org/10.1007/s00394-017-1524-x.

[12] J. Petrasek, T. Csak, G. Szabo, Toll-like receptors in liver disease, Adv. Clin. Chem. 59 (2013) 155–201.

[13] H.C. Huang, Y.I. Weng, C.R. Lee, T.R. Jan, Y.L. Chen, Y.T. Lee, Protection by scoparone against the alterations of plasma lipoproteins, vascular morphology and vascular reactivity in hyperlipidaemic diabetic rabbit, Br. J. Pharmacol. 110 (4) (1993) 1508–1514.

[14] J.K. Kim, J.Y. Kim, H.J. Kim, K.G. Park, R.A. Harris, W.J. Cho, I.K. Lee, Scoparone exerts anti-tumor activity against DU145 prostate cancer cells via inhibition of STAT3 activity, PLoS One 8 (11) (2013) e80391, , https://doi.org/10.1371/journal.pone.0080391.

[15] D.Y. Cho, H.M. Ko, J. Kim, B.W. Kim, Y.S. Yun, J.I. Park, D.K. Choi, Scoparone inhibits LPS-simulated inflammatory response by suppressing IRF3 and ERK in BV-2 microglial cells, Molecules (Basel, Switzerland) 21 (12) (2016), https://doi.org/10.3390/molecules21121718.

[16] C. Lu, Y. Li, S. Hu, Y. Cai, Z. Yang, K. Peng, Scoparone prevents IL-1beta-induced inflammatory response in human osteoarthritis chondrocytes through the PI3K/Akt/NF-kappaB pathway, Biomed. Pharmacother. = Biomedecine & Pharmacotherapie 106 (2018) 1169–1174, https://doi.org/10.1016/j.biopha.2018.07.062.

[17] H.C. Huang, C.R. Lee, Y.I. Weng, M.C. Lee, Y.T. Lee, Vasodilator effect of scoparone (6,7-dimethoxycoumarin) from a Chinese herb, Eur. J. Pharmacol. 218 (1) (1992) 123–128.

[18] H.Y. Hung, S.C. Kuo, Recent studies and progression of Yin Chen Hao (Yin Chen Hao), a long-term used traditional Chinese medicine, J. Tradit. Complement. Med. 3 (1) (2013) 2–6, https://doi.org/10.4103/2225-4110.106533.

[19] A. Zhang, H. Sun, S. Dou, W. Sun, X. Wu, P. Wang, X. Wang, Metabolomics study on the hepatoprotective effect of scoparone using ultra-performance liquid chromatography/electrospray ionization quadruple time-of-flight mass spectrometry, Analyst 138 (1) (2013) 353–361, https://doi.org/10.1039/c2an36382h.

[20] A. Zhang, H. Sun, X. Wang, Urinary metabolic profiling of rat models revealed protective function of scoparone against alcohol induced hepatotoxicity, Sci. Rep. 4 (2014) 6768, , https://doi.org/10.1038/srep06768.

[21] A. Zhang, H. Sun, G. Wu, W. Sun, Y. Yuan, X. Wang, Proteomics analysis of hepatoprotective effects for scoparone using MALDI-TOF/TOF mass spectrometry with bioinformatics, Omics J. Integr. Biol. 17 (4) (2013) 224–229, https://doi.org/10.1089/omi.2012.0064.

[22] D. Yang, J. Yang, D. Shi, R. Deng, B. Yan, Scoparone potentiates transactivation of the bile salt export pump gene and this effect is enhanced by cytochrome P450 metabolism but abolished by a PKC inhibitor, Br. J. Pharmacol. 164 (5) (2011) 1547–1557, https://doi.org/10.1111/j.1476-5381.2011.01522.x.

[23] X. Liu, X. Zhao, Scoparone attenuates hepatic stellate cell activation through inhibiting TGF-beta/Smad signaling pathway, Biomed. Pharmacother. = Biomedecine & Pharmacotherapie 93 (2017) 57–61, https://doi.org/10.1016/j.biopha.2017.06.006.

[24] Q. Yin, H. Sun, A. Zhang, X. Wang, Pharmacokinetics and tissue distribution study of scoparone in rats by ultraperformance liquid-chromatography with tandem high-definition mass spectrometry, Fitoterapia 83 (4) (2012) 795–800, https://doi.org/10.1016/j.fitote.2012.03.010.

[25] Q. Chen, A. Boire, X. Jin, M. Valiente, E.E. Er, A. Lopez-Soto, J. Massague, Carcinoma-astrocyte gap junctions promote brain metastasis by cGAMP transfer, Nature 533 (7604) (2016) 493–498, https://doi.org/10.1038/nature18268.

[26] K. Sato, X. Feng, J. Chen, J. Li, P. Muranski, M.J. Desierto, N.S. Young, PPARgamma antagonist attenuates mouse immune-mediated bone marrow failure by inhibition of T cell function, Haematologica 101 (1) (2016) 57–67, https://doi.org/10.3324/haematol.2014.121632.

[27] Y. Takahashi, T. Fukusato, Histopathology of nonalcoholic fatty liver disease/nonalcoholic steatohepatitis, World J. Gastroenterol. 20 (42) (2014) 15539–15548, https://doi.org/10.3748/wjg.v20.i42.15539.

[28] D.E. Kleiner, E.M. Brunt, M. Van Natta, C. Behling, M.J. Contos, O.W. Cummings, A.J. Sanyal, Design and validation of a histological scoring system for nonalcoholic fatty liver disease, Hepatology 41 (6) (2005) 1313–1321, https://doi.org/10.1002/hep.20701.

[29] X. Deng, X. Pan, C. Cheng, B. Liu, H. Zhang, Y. Zhang, K. Xu, Regulation of SREBP-2 intracellular trafficking improves impaired autophagic flux and alleviates endoplasmic reticulum stress in NAFLD, Biochim. Biophys. Acta 1862 (3) (2017) 337–350, https://doi.org/10.1016/j.bbalip.2016.12.007.

[30] M. Hatting, G. Zhao, F. Schumacher, G. Sellge, M. Al Masaoudi, N. Gabetaler, C. Trautwein, Hepatocyte caspase-8 is an essential modulator of steatohepatitis in rodents, Hepatology 57 (6) (2013) 2189–2201, https://doi.org/10.1002/hep.26271.

[31] F. Tacke, H.W. Zimmermann, Macrophage heterogeneity in liver injury and fibrosis, J. Hepatol. 60 (5) (2014) 1090–1096, https://doi.org/10.1016/j.jhep.2013.12.025.

[32] T. Sharifnia, J. Antoun, T.G. Verriere, G. Suarez, J. Wattacheril, K.T. Wilson, C.R. Flynn, Hepatic TLR4 signaling in obese NAFLD, Am. J. Physiol. Gastrointest. Liver Physiol. 309 (4) (2015) G270–G278, https://doi.org/10.1152/ajpgi.00304.2014.

[33] O. Krenkel, T. Puengel, O. Govaere, A.T. Abdallah, J.C. Mossanen, M. Kohlhepp, F. Tacke, Therapeutic inhibition of inflammatory monocyte recruitment reduces steatohepatitis and liver fibrosis, Hepatology 67 (4) (2018) 1270–1283, https://doi.org/10.1002/hep.29544.

[34] P.J. Murray, Macrophage polarization, Annu. Rev. Physiol. 79 (2017) 541–566, https://doi.org/10.1146/annurev-physiol-022516-034339.

[35] Y. Takahashi, Y. Soejima, T. Fukusato, Animal models of nonalcoholic fatty liver disease/nonalcoholic steatohepatitis, World J. Gastroenterol. 18 (19) (2012) 2300–2308, https://doi.org/10.3748/wjg.v18.i19.2300.
[36] L. Hebbard, J. George, Animal models of nonalcoholic fatty liver disease, Nat. Rev. Gastroenterol. Hepatol. 8 (1) (2011) 35–44, https://doi.org/10.1038/nrgastro.2010.191.
[37] J.R. Noh, Y.H. Kim, J.H. Hwang, G.T. Gang, S.H. Yeo, K.S. Kim, C.H. Lee, Scoparone inhibits adipocyte differentiation through down-regulation of peroxisome proliferators-activated receptor gamma in 3T3-L1 preadipocytes, Food Chem. 141 (2) (2013) 723–730, https://doi.org/10.1016/j.foodchem.2013.04.036.
[38] A. Dela Pena, I. Leclercq, J. Field, J. George, B. Jones, G. Farrell, NF-kappaB activation, rather than TNF, mediates hepatic inflammation in a murine dietary model of steatohepatitis, Gastroenterology 129 (5) (2005) 1663–1674, https://doi.org/10.1053/j.gastro.2005.09.004.
[39] F. Marra, Nuclear factor-kappaB inhibition and non-alcoholic steatohepatitis: inflammation as a target for therapy, Gut 57 (5) (2008) 570–572, https://doi.org/10.1136/gut.2007.141986.
[40] R. Wu, G. Nakatsu, X. Zhang, J. Yu, Pathophysiological mechanisms and therapeutic potentials of macrophages in non-alcoholic steatohepatitis, Expert Opin. Ther. Targets 20 (5) (2016) 615–626, https://doi.org/10.1517/14728222.2016.1125883.
[41] L. Zhang, D. Schuppan, Traditional Chinese Medicine (TCM) for fibrotic liver disease: hope and hype, J. Hepatol. 61 (1) (2014) 166–168, https://doi.org/10.1016/j.jhep.2014.03.009.
[42] F. Salamone, F. Galvano, F. Cappello, A. Mangiameli, I. Barbagallo, G. Li Volti, Silibinin modulates lipid homeostasis and inhibits nuclear factor kappa B activation in experimental nonalcoholic steatohepatitis, Transl. Res. J. Lab. Clin. Med. 159 (6) (2012) 477–486, https://doi.org/10.1016/j.trsl.2011.12.003.
[43] R. Li, J. Li, Y. Huang, H. Li, S. Yan, J. Lin, T. Lan, Polydatin attenuates diet-induced nonalcoholic steatohepatitis and fibrosis in mice, Int. J. Biol. Sci. 14 (11) (2018) 1411–1425, https://doi.org/10.7150/ijbs.26086.
[44] Y. Cheng, T. Chen, J. Ping, J. Chen, Cangju Qinggan Jiangzhi decoction reduces the development of nonalcoholic steatohepatitis and activation of Kupffer cells, Cell. Physiol. Biochem. Int. J. Exp. Cell. Physiol. Biochem. Pharmacol. 48 (3) (2018) 971–982, https://doi.org/10.1159/000491965.
[45] J. Zhang, H. Zhang, X. Deng, N. Zhang, B. Liu, S. Xin, K. Xu, Baicalin attenuates non-alcoholic steatohepatitis by suppressing key regulators of lipid metabolism, inflammation and fibrosis in mice, Life Sci. 192 (2018) 46–54, https://doi.org/10.1016/j.lfs.2017.11.027.
[46] C. Wah Kheong, N.R. Nik Mustapha, S. Mahadeva, A randomized trial of silymarin for the treatment of nonalcoholic steatohepatitis, Clin. Gastroenterol. Hepatol. Off. Clin. Pract. J. Am. Gastroenterol. Assoc. 15 (12) (2017) 1940–1949.e1948, https://doi.org/10.1016/j.cgh.2017.04.016.
[47] X. Ni, H. Wang, Silymarin attenuated hepatic steatosis through regulation of lipid metabolism and oxidative stress in a mouse model of nonalcoholic fatty liver disease (NAFLD), Am. J. Transl. Res. 8 (2) (2016) 1073–1081.
[48] J.G. Fan, L. Wei, H. Zhuang, Guideline of prevention and treatment of nonalcoholic fatty liver disease (2018, China), J. Dig. Dis. (2018), https://doi.org/10.1111/1751-2980.12685.
[49] K. Kazankov, S.M.D. Jorgensen, The role of macrophages in nonalcoholic fatty liver disease and nonalcoholic steatohepatitis, Nat Rev Gastroenterol Hepatol. 16 (3) (2019) 145–159, https://doi.org/10.1038/s41575-018-0082-x.